Analytical Methods

Accepted Manuscript

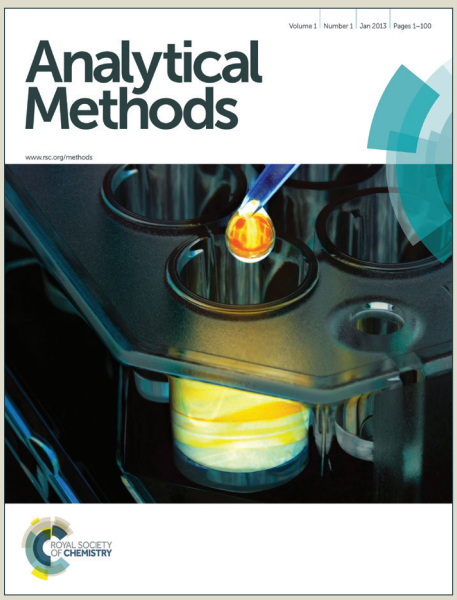

ROYAL SOCIETY OF CHEMISTRY

www.rsc.org/methods

Journal Name

RSCPublishing

ARTICLE

Trace Detection and Competitive Ionization of Erythritol Tetranitrate in Mixtures Using Direct Analysis in Real Time Mass Spectrometry†‡

Thomas P. Forbes* and Edward Sisco

Cite this: DOI: 10.1039/xoxxoooooox

Received ooth January 2012,
Accepted ooth January 2012

DOI: 10.1039/xoxxoooooox

www.rsc.org/

Direct analysis in real time (DART) mass spectrometry (MS) was used for trace detection of the nitrate ester explosive erythritol tetranitrate (ETN) and its sugar alcohol precursor erythritol. The present investigation revealed the impact of competitive ionization between ETN, erythritol, and nitric acid for the detection of sugar alcohol-based homemade explosives. DART-MS facilitated the direct investigation of matrix effects related to the desorption process and compound volatility, as well as the ionization process, neutralization, and affinity for nitrate adduct formation. ETN and erythritol were directly detected at nanogram to sub-nanogram levels by DART-MS.

Introduction

The sensitive detection of explosive compounds and identification of explosive device signatures remains an area of importance. Ion mobility spectrometry (IMS) has provided rapid trace detection with readily field deployable instruments.[1-3] However, IMS lacks the specificity of mass spectrometric techniques for in-depth analysis of ion chemistries and desorption phenomena. Alternative detection schemes such as gas chromatography mass spectrometry (GC/MS)[4, 5] or liquid chromatography (LC/MS)[6, 7] are hindered by lengthy analysis times. The combination of mass spectrometry's (MS) superior selectivity and sensitivity as well as recent advancements in ambient ionization techniques such as desorption electrospray ionization (DESI)[8] and direct analysis in real time (DART),[9] have delivered appealing alternatives.[10] These desorption-based ambient ionization methods enable the direct analysis of analytes from a variety of surfaces with no or minimal sample preparation. Trace detection of a range of explosive compounds directly from paper, metals, plastics, and human skin has been demonstrated with DESI-MS.[11-13] DESI and other liquid droplet-based ambient ionization sources[14] ionize explosive compounds through the traditional mechanisms studied for electrospray ionization (ESI),[15, 16] forming adducts with available nitrite (NO_2^-), nitrate (NO_3^-), or reactive species added to the spray solvent (Cl^-). Similarly, the plasma-based DART source has demonstrated explosives detection by ionization through the production of He metastable atoms, which are hypothesized to initiate Penning ionization of atmospheric water, and subsequently ionize analytes desorbed by the heated gas stream.[4, 17-19] Prior investigations have also demonstrated the use of dopants for enhanced ionization and specific adduct formation with DART.[4, 20]

The focus of most explosives detection investigations has been on military-grade nitrated organic explosives, generally nitroaromatics (trinitrotoluene, TNT), nitramines (cyclotrimethylenetrinitramine, RDX), and select nitrate esters (pentaerythritol tetranitrate, PETN).[3, 9, 11-13, 18, 21] As the threats posed by homemade and improvised explosive devices (HMEs/IEDs) increase, trace detection of primary explosives such as fuel-oxidizer mixtures and peroxides (triacetone triperoxide, TATP; hexamethylene triperoxide diamine, HMTD; and hexamethylene diperoxide diamine, HMDD) has become a growing area of research in recent years.[21-24] In the present study, we focus on homemade nitrate esters based on the nitration of sugar alcohol, or polyol, precursors (Scheme 1). Specifically, we investigated the trace detection and competitive ionization of the 4-carbon sugar alcohol erythritol, the commercial alternative sweetener Truvia®, and the nitrate ester erythritol tetranitrate (ETN) using direct analysis in real time mass spectrometry (DART-MS). We demonstrated the detection limits for each analyte as well as the competitive ionization effects of detection from a mixture.

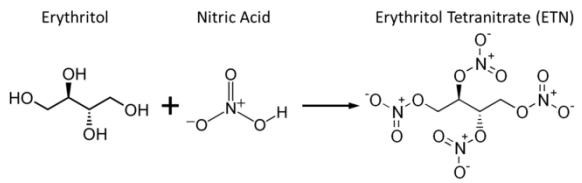

Scheme 1 Nitration of the sugar alcohol erythritol for fabrication of the nitrate ester explosive, erythritol tetranitrate (ETN).

Experimental Methods

Materials and Sample Preparation

The explosive standard erythritol tetranitrate was obtained from AccuStandard (New Haven, CT, USA) at 1 mg/mL in acetonitrile.§ Erythritol and Truvia were purchased from Sigma-Aldrich (St. Louis, MO, USA) and obtained from the cafeteria, respectively, and dissolved/diluted in liquid chromatography-mass spectrometry (LC-MS) Ultra Chromasolv grade methanol (Sigma-Aldrich) The nitrate ester and sugar alcohols were further diluted in acetonitrile and methanol, respectively. Serial dilutions were used for limit of detection measurements. The Truvia nutrition facts reported 3 g of erythritol per 3.5 g Truvia. Samples were deposited onto and detected from polytetrafluoroethylene (PTFE, Teflon) substrates (Tekdon, Inc., Myakka City, FL, USA) for limit of detection and competitive ionization investigations. Nomex® (Smiths Detection, Hertfordshire, UK) and PTFE-coated fiberglass weave (DSA Detection, North Andover, MA, USA) swabs were also used for analyte collection from primary surfaces such as machined aluminum, with a single continuous swiping motion.

Instrumentation

Desorption and ionization were achieved with a DART ion source (IonSense, Saugus, MA, USA) coupled to an orthogonal time-of-flight mass spectrometer (AccuTOF™, JEOL USA, Inc., Peabody, MA, USA) by a Vapur® hydrodynamic-assist interface (IonSense, Saugus, MA, USA). The DART source was incorporated in an off-axis desorption-style configuration, similar to configurations used for liquid droplet-based desorption ionization sources.[8, 13, 23] The experimental geometry consisted of the DART source at a 45° angle with respect to sample surface, 10 mm orthogonal distance from DART tip to Vapur interface inlet, 5 mm orthogonal distance from DART tip to sample substrate, and 1 mm distance from sample substrate to Vapur interface inlet. The helium gas, at a flow rate of 1.5 L/min and heated to 300 °C, was ionized by a –3000 V potential applied to the needle electrode. Experiments were conducted with the following AccuTOF™ mass spectrometer parameters: 100 °C orifice temperature, -20 V orifice 1 voltage, -5 V ring lens voltage, -5 V orifice 2 voltage, and -400 V peaks voltage. Mass spectra were acquired from *m/z* 40 to *m/z* 800 at a rate of 0.5 s/scan. The Vapur® interface improves transfer efficiency into the mass spectrometer inlet by hydrodynamically pulling vacuum through the Vapur inlet at 3.8 L/min with a rough pump. Polyethylene glycol 400 (PEG 400) was used as the MS tuning compound, diluted in methanol.

Cumulative Intensity Distributions

The temporal response of each ionization pathway under various conditions was quantified by the time constant of cumulative intensity distributions. Cumulative distributions were derived from each extracted ion chronogram (Fig. S1) and curve fitted with MATLAB (Version R2013a, The Mathworks, Inc., Natick, MA, USA) to the functional form: $f(x) = a(1 - e^{-x/\tau}) + b$. Here, τ was defined as the time constant for each molecule's respective ionization pathways. Normalization of the cumulative distributions enabled direct comparison of the temporal response of each ionization pathway for the various conditions investigated.

Results and Discussion

Fig. 1 shows the negative ion mode mass spectrum for a mixture of Truvia and ETN collected with a dry Nomex swab from a machined aluminum surface. Many common operating procedures for the forensic collection of trace analytes are centered on dry swab collection. For this demonstration, 500 ng of each analyte were independently deposited onto the aluminum substrate and collected in a single continuous swiping motion. Significant ETN ($C_4H_6N_4O_{12}$) adducts were identified by accurate mass, corresponding to the nitrate adduct *m/z* 363.986 $[ETN+NO_3]^-$, the dimer nitrate adduct *m/z* 665.984 $[2ETN+NO_3]^-$, and an adduct ion with the background peak of *m/z* 76.987 $[CO_2OOH]^-$, yielding *m/z* 378.986 $[ETN+CO_2OOH]^-$. Less abundant ETN ions for the loss of a nitrite *m/z* 256.005 $[ETN-NO_2]^-$ and hydroxide adduct *m/z* 319.001 $[ETN+OH]^-$ were also observed. Erythritol was recognized as the main component of the Truvia alternative sweetener and the deprotonated ion, *m/z* 121.050 $[M-H]^-$, dominated its ion distribution with less abundant ions observed for the nitrite adduct, *m/z* 168.051 $[M+NO_2]^-$, nitrate adduct, *m/z* 184.046 $[M+NO_3]^-$, and the deprotonated dimer, *m/z* 243.108 $[2M-H]^-$. Here and throughout this investigation, "M" will refer to erythritol ($C_4H_{10}O_4$). Similar ion distributions were observed for a Truvia – ETN mixture collected with a PTFE-coated fiberglass weave swab (Fig. S2, ESI†). While detected in positive ion mode, both the sugar alcohol and nitrate ester demonstrated superior performance and improved sensitivity in negative mode.

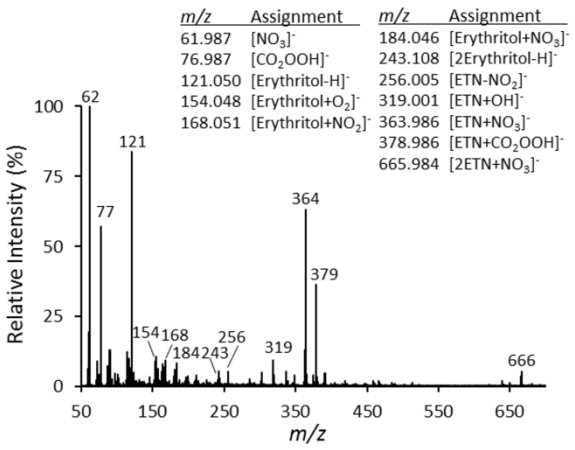

Fig. 1 Representative DART negative ion mode mass spectrum of an erythritol tetranitrate (ETN) – Truvia mixture collected with a Nomex swab from an aluminum substrate. Peak assignments are listed in figure.

Table 1 Limit of detection analysis of nitrate ester explosive and sugar alcohol precursors by DART-MS

Compound	Ion Observed	LOD	S/N at LOD
ETN	$[ETN + NO_3]^-$	2 ng	7 : 1
Erythritol (pure)	[Erythritol - H]$^-$	250 pg	4 : 1
Erythritol (Truvia)[a]	[Erythritol - H]$^-$	1 ng	5 : 1

[a] LOD of Truvia reflects the approximate mass of erythritol within Truvia mixture (0.857 g erythritol per 1 g Truvia)

Approximate limits of detection (LOD) for the nitrate ester explosive, ETN, pure erythritol, and erythritol within the alternative sweetener Truvia were measured. Table 1 summarizes the major ion observed, the LOD, and the signal-to-noise (S/N) ratio at the LOD. Measurements were taken in triplicate from a PTFE substrate, samples were interrogated to depletion, and the resulting LODs denote the deposited mass of analyte. The noise level was identified as three standard deviations above the background level. The final S/N was calculated by the AccuTOF™ software (Mass Center Main). Although no significant peaks were identified for other Truvia ingredients, the detection limit for pure erythritol was approximately 4-fold better than erythritol from the alternative sweetener mixture.

The trace detection of explosives and explosive device signatures may often require detection from mixtures of the explosive with precursors, by-products, and environmental contaminants. We consider the detection and competitive ionization of ETN in the presence of its precursors, erythritol (in the form of Truvia) and nitric acid (Scheme 1). In addition, we investigated the effects of acetone vapor, a common dopant for DART ionization enhancement.[4, 20] Fig. 2 displays representative extracted ion chronograms (EICs) for a number of the dominant erythritol and ETN adducts for nine test cases. The mixtures investigated were (A) 0 ng ETN – 50 ng erythritol (all erythritol in the form of Truvia), (B) 50 ng ETN – 0 ng erythritol, and (C) 50 ng ETN – 50 ng erythritol; each in the presence of (1) no additives, (2) 5 µL of 0.005 % HNO_3, and (3) acetone vapor. The main ions for both erythritol ([M-H]$^-$, $[M+NO_2]^-$, and $[M+NO_3]^-$) and ETN ($[ETN+NO_3]^-$ and $[ETN+CO_2OOH]^-$) demonstrated similar temporal responses when interrogated individually, with the volatile ETN adducts decaying quicker (Fig. 2(1A) and 2(1B)). However, for an erythritol/ETN mixture, competitive ionization, neutralization effects, and the effects of their different volatility characteristics were observed. Both the deprotonated erythritol ion and erythritol nitrite adduct revealed a delay in their temporal responses, *i.e.*, time constant (Fig. 2(1C)). Representative mass spectra from a number of test cases and time points are shown in Figure 3.

Fig. 4 displays (a) the peak area and (b) time constant of the cumulative signal distribution (temporal response) for a number of the main erythritol and ETN ions (Fig. S1, ESI†). The data and uncertainty represent the average and standard deviation for 4 replicate samples. As the mixture was introduced into the heated helium metastable jet from the DART source, the

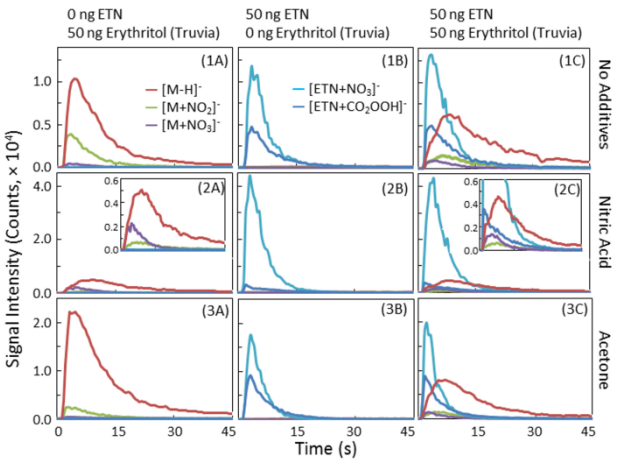

Fig. 2 Representative DART extracted ion chronograms for mixture compositions (A) 0 ng ETN – 50 ng erythritol, (B) 50 ng ETN – 0 ng erythritol, and (C) 50 ng ETN – 50 ng erythritol, in the presence of (1) no additives, (2) 5 µL of 0.005 % HNO_3, and (3) acetone vapor.

majority of the more volatile ETN desorbed first, along with some fraction of the less volatile erythritol. During this initial period, the acidic ETN acted as a proton donor and source of nitrate ions. The abundance of this species led to the neutralization of some fraction of the deprotonated erythritol ions, [M-H]$^-$, and an increase adduct formation with nitrate, $[M+NO_3]^-$. Following the surge in ETN desorption, the ETN signal quickly decayed, depleting in 10 s to 15 s. However, the less volatile erythritol continued to desorb for an additional 15 s to 30 s beyond the ETN depletion. With the nitrate source and proton donor (ETN) exhausted, the dominant observed ionization pathway transitioned from the nitrate adduct to the deprotonated ion [M-H]$^-$. Fig. 3(a) and 3(b) display representative negative ion mode mass spectra at times associated with the peak in the ETN nitrate adduct and the deprotonated erythritol ion signals, respectively. The presence of erythritol did not significantly (Student's *t* test, $P > 0.2$) affect the ETN signal abundance due to competition for the available nitrate ions (Fig. 5(a)). In addition, due to the combination of their respective volatilities, affinity for nitrate,

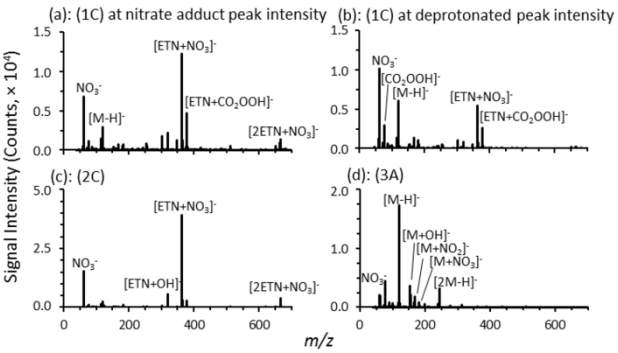

Fig. 3 Representative DART mass spectra for mixture compositions of (a) test case (1C) at the nitrate adduct peak intensity, (b) test case (1C) at the deprotonated erythritol peak intensity, (c) test case (2C), and (d) test case (3A). "M" represents erythritol in the figure.

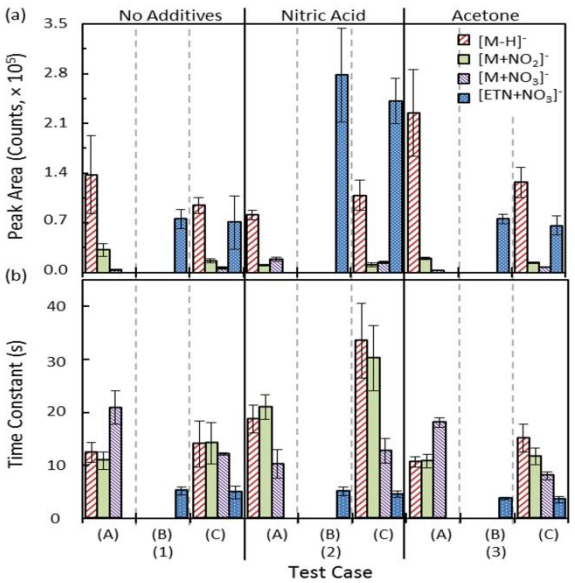

Fig. 4 (a) Integrated peak area as function of test case for erythritol: *m/z* 121.050 $[M\text{-}H]^-$, *m/z* 168.051 $[M+NO_2]^-$, *m/z* 184.046 $[M+NO_3]^-$; and ETN: *m/z* 363.986 $[ETN+NO_2]^-$. "M" represents erythritol in the figure and caption. (b) Time constant for cumulative signal distribution of respective ion. Test case mixture compositions: (A) 0 ng ETN – 50 ng erythritol, (B) 50 ng ETN – 0 ng erythritol, and (C) 50 ng ETN – 50 ng erythritol; (1) no additives, (2) with 5 µL of 0.005 % HNO_3, and (3) in the presence of acetone vapor. Data bars and uncertainty expressed as the average and standard deviations, respectively, for 4 replicate successive samples.

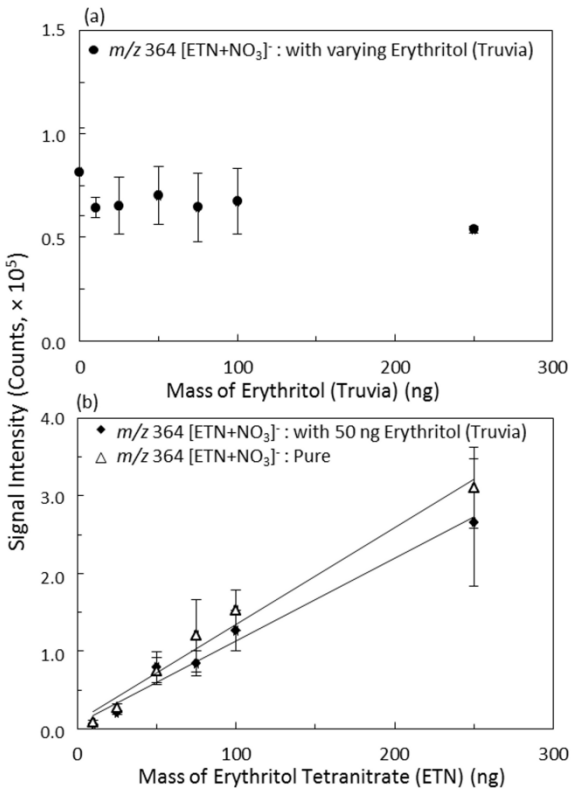

Fig. 5 Integrated peak area of the ETN nitrate adduct, *m/z* 363.986 $[ETN+NO_3]^-$, for (a) 50 ng of ETN as a function of erythritol mass of 0 ng to 250 ng, and (b) for increasing amounts of ETN from 10 ng to 250 ng in the presence of 50 ng of erythritol. Data points and uncertainty represented as the average and standard deviation, respectively, for 4 replicate samples.

and acidity ETN's sensitivity remained constant for further increases in the erythritol present (up to 250 ng erythritol investigated, Fig. 5(a)). This minimal effect on the ETN ionization was also demonstrated in the linear response of ETN from 10 ng to 250 ng in the presence of 50 ng erythritol (in the form of Truvia, Fig. 5(b)).

The relative volatility of ETN/erythritol, competitive ionization, neutralization effects, and affinity for nitrate adduct formation were further investigated in the presence of nitric acid (HNO_3), another precursor for multiple fabrication pathways of ETN and an inorganic source of free nitrate ions. As alluded to by erythritol's neutralization in the presence of the proton donor, ETN, the temporal response for erythritol alone in the presence of nitric acid experienced a similar, and more pronounced, initial elevation in signal abundance of the erythritol nitrate adduct (Fig. 2(2A) and S1(2A)). This elevation in nitrate adduct formation also corresponded to temporal delays in the deprotonated ion and nitrite adduct pathways (Fig. 4). Similar to the desorption/ionization processes in the presence of ETN, nitric acid acted as a proton donor, neutralization the deprotonated ion during the initial desorption time period. Unlike ETN, nitric acid itself consumed no nitrate ions and its higher volatility provided the rapid introduction of protons and nitrate ions (Fig. 4(b)). As expected, ETN in the presence of nitric acid led to a substantial increase in the nitrate adduct signal. However, the mixture of both in the presence of nitric acid led to a slight decrease in the signal abundance of the ETN nitrate adduct as it competes with erythritol for available nitrates (Fig. 4). In addition, the presence of two proton donors and nitrate sources further demonstrated the neutralization of the deprotonated erythritol ion and increased observation of the nitrate adduct. After the depletion of these more volatile compounds (ETN and nitric acid) the ionization pathways resulting in deprotonation and nitrite adduct formation were again observed.

Finally, we considered the series again in the presence of acetone vapor, a dopant for DART ionization enhancement of certain compounds through proton transfer.[20] The high gas-phase basicity of acetone boosted proton transfer and increased the signal abundance of the deprotonated erythritol ion, $[M\text{-}H]^-$ (Figs. 3(d) and 4). The deprotonated ion also experienced a slight decrease in response time (Fig. 4(b)). However, deprotonation represented only a minor ionization pathway for ETN, and therefore acetone did not provide significant improvement for the detection of ETN (Figs. 2(3B) and 4(a)). Although acetone boosted the deprotonation of erythritol, in the mixture of ETN and erythritol, ETN again acted as a proton donor and source of nitrate. Similar to above, the deprotonated erythritol ions were neutralized and nitrate adducts formed during the lifetime of the ETN signal.

Conclusions

The trace detection of explosives from complex mixtures remains of utmost importance. The results obtained here demonstrated the trace detection and competitive ionization of erythritol tetranitrate in mixtures containing its precursors, erythritol – in the form of the alternative sweetener Truvia – and nitric acid, using DART-MS. This rapid desorption/ionization technique enabled detection of these components at nanogram to sub-nanogram levels with no sample preparation or treatment. The higher volatility and stronger nitrate affinity of ETN resulted in no significant decrease in signal abundance from competitive ionization in the presence of its sugar alcohol precursor, erythritol.

Acknowledgements

The U.S. Department of Homeland Security Science and Technology Directorate sponsored a portion of the production of this material under Interagency Agreement IAA HSHQDC-12-X-00024 with the National Institute of Standards and Technology. The authors thank Dr. Chris Szakal and Dr. Shin Muramoto at the National Institute of Standards and Technology (NIST) for stimulating discussion.

Notes and references

National Institute of Standards and Technology, Materials Measurement Science Division, Gaithersburg, Maryland 20899, United States. E-mail: thomas.forbes@nist.gov

† Electronic Supplementary Information (ESI) available: Additional mass spectra and figures. See DOI: 10.1039/c000000x/

‡ Official contribution of the National Institute of Standards and Technology; not subject to copyright in the United States.

§ Certain commercial products are identified in order to adequately specify the procedure; this does not imply endorsement or recommendation by NIST, nor does it imply that such products are necessarily the best available for the purpose.

1. R. G. Ewing, D. A. Atkinson, G. A. Eiceman and G. J. Ewing, *Talanta*, 2001, **54**, 515-529.
2. B. M. Kolakowski and Z. Mester, *Analyst*, 2007, **132**, 842-864.
3. M. Najarro, M. E. Davila Morris, M. E. Staymates, R. Fletcher and G. Gillen, *Analyst*, 2012, **137**, 2614-2622.
4. E. Sisco, J. Dake and C. Bridge, *Forensic Sci. Int.*, 2013, **232**, 160-168.
5. A. Halasz, C. Groom, E. Zhou, L. Paquet, C. Beaulieu, S. Deschamps, A. Corriveau, S. Thiboutot, G. Ampleman, C. Dubois and J. Hawari, *J. Chromatogr., A.*, 2002, **963**, 411-418.
6. C. N. McEwen, R. G. McKay and B. S. Larsen, *Anal. Chem.*, 2005, **77**, 7826-7831.
7. D. Perret, S. Marchese, A. Gentili, R. Curini, A. Terracciano, E. Bafile and F. Romolo, *Chromatographia*, 2008, **68**, 517-524.
8. Z. Takáts, J. M. Wiseman, B. Gologan and R. G. Cooks, *Science*, 2004, **306**, 471-473.
9. R. B. Cody, J. A. Laramée and H. D. Durst, *Anal. Chem.*, 2005, **77**, 2297-2302.
10. R. G. Cooks, Z. Ouyang, Z. Takats and J. M. Wiseman, *Science*, 2006, **311**, 1566-1570.
11. D. R. Justes, N. Talaty, I. Cotte-Rodriguez and R. G. Cooks, *Chem. Commun.*, 2007, 2142-2144.
12. C. Szakal and T. M. Brewer, *Anal. Chem.*, 2009, **81**, 5257-5266.
13. Z. Takats, I. Cotte-Rodriguez, N. Talaty, H. Chen and R. G. Cooks, *Chem. Commun.*, 2005, 1950-1952.
14. T. P. Forbes, T. M. Brewer and G. Gillen, *Analyst*, 2013, **138**, 5665-5673.
15. M. Dole, L. L. Mack, R. L. Hines, R. C. Mobley, L. D. Ferguson and M. B. Alice, *J. Chem. Phys.*, 1968, **49**, 2240-2249.
16. J. V. Iribarne and B. A. Thomson, *J. Chem. Phys.*, 1976, **64**, 2287-2294.
17. G. A. Harris, C. E. Falcone and F. M. Fernández, *J. Am. Soc. Mass Spectrom.*, 2012, **23**, 153-161.
18. J. M. Nilles, T. R. Connell, S. T. Stokes and H. Dupont Durst, *Propell., Explos., Pyrot.*, 2010, **35**, 446-451.
19. E. Sisco and T. P. Forbes, *Analyst*, 2015, DOI:10.1039/C1034AN02347A.
20. L. Song, A. B. Dykstra, H. Yao and J. E. Bartmess, *J. Am. Soc. Mass Spectrom.*, 2009, **20**, 42-50.
21. J. F. Garcia-Reyes, J. D. Harper, G. A. Salazar, N. A. Charipar, Z. Ouyang and R. G. Cooks, *Anal. Chem.*, 2010, **83**, 1084-1092.
22. I. Cotte-Rodriguez, H. Chen and R. G. Cooks, *Chem. Commun.*, 2006, 953-955.
23. T. P. Forbes and E. Sisco, *Anal. Chem.*, 2014, **86**, 7788-7797.
24. S. Parajuli and W. Miao, *Anal.Chem.*, 2013, **85**, 8008-8015.